

Improved lifetime of a high spin polarization superlattice photocathode

Jai Kwan Bae, Alice Galdi, Luca Cultrera, Frank Ikponmwen, Jared Maxson, and Ivan Bazarov

Cornell Laboratory for Accelerator-Based Sciences and Education, Cornell University, Ithaca, NY 14853, USA

(Dated: 22 November 2019)

Negative Electron Affinity (NEA) activated surfaces are required to extract highly spin polarized electron beams from GaAs-based photocathodes, but they suffer extreme sensitivity to poor vacuum conditions that results in rapid degradation of quantum efficiency. We report on series of unconventional NEA activations on surfaces of bulk GaAs with Cs, Sb, and O₂ using different methods of oxygen exposure for optimizing photocathode performance. One order of magnitude improvement in lifetime with respect to the standard Cs-O₂ activation is achieved without significant loss on electron spin polarization and quantum efficiency by codepositing Cs, Sb, and O₂. A strained GaAs/GaAsP superlattice sample activated with the codeposition method demonstrated similar enhancement in lifetime near the photoemission threshold while maintaining 90% spin polarization.

I. INTRODUCTION

Highly spin polarized electron beams with high currents are required by future nuclear physics facilities such as the Electron Ion Collider and the International Linear Collider.¹⁻³ Photocathode sources capable of providing spin polarized electron beams at high currents (~ 50 mA)⁴ for extended period of time which are robust against less than ideal vacuum conditions are required in order to reduce the cost and complexity of operating these new facilities. Long lifetime polarized electron sources are also of interest for electron microscopy technologies that exploits spin polarization to probe magnetization in materials and nanostructures at the nanoscale level. Additionally, bright spin polarized sources driven with a short pulse laser can enable time studies of magnetization dynamics.⁵⁻⁷ GaAs-based photocathodes are the present state of the art for the spin polarized electron sources because they can provide highly spin polarized electron beams with high efficiency.⁸ However, their short operational lifetime poses limits particularly for applications requiring high average current.⁹

GaAs was first shown to be an attractive electron photoemitter five decades ago via the discovery of negative electron affinity (NEA) activation on *p*-type samples.¹⁰ When the GaAs surface is exposed to cesium vapor (electropositive metal atoms), a strong dipole layer is formed on the surface that lowers the electron affinity, which is defined as the energy difference between the vacuum level and conduction band minimum.¹¹ If the GaAs is *p*-doped, the effective electron affinity can become negative because of the downward band bending near the surface. Thus, in NEA conditions, electrons that have relaxed down to the bottom of the conduction band after photoexcitation can still escape into vacuum when they reach the vacuum interface. The combination of NEA and other characteristics of GaAs-based photocathodes, such as high electron mobility, results in a high quantum efficiency (QE) at the band gap photon energy of about 1.4 eV.¹² Later, it was demonstrated that the introduction of an oxidant, such as oxygen or NF₃, during cesiation can yield an even stronger dipole moment layer and achieve larger NEA and hence larger QE.^{13,14}

Spin polarized electron photoemission from GaAs is achieved by exploiting the quantum mechanical selection rule that conserves the total angular momentum during photoexcitation with circularly polarized light.¹² Since electrons need to be excited only from the top of the valence band for a high spin polarization, NEA is required. Due to the degenerate light-hole and heavy-hole band states in the P_{3/2} valence band, the theoretical limit of spin polarization of NEA bulk GaAs is 50%. Additionally, various spin relaxation mechanisms

limit spin polarization from bulk GaAs to $\sim 35\%$ at room temperature.¹¹ A number of approaches have been proposed to overcome this limit,^{15,16} where exerting lattice strain on GaAs aimed at breaking the valence band degeneracy has been the most successful. This method exhibits a high spin polarization of 90%, but suffers from significantly decreased QE of 0.07%.¹⁷ In an extension of this approach, GaAs/GaAsP multi-layer superlattices structures with a distributed Bragg reflector were shown to improve the QE up to 6.4% with a spin polarization of 84%.⁸

NEA surface of GaAs suffers from extreme vacuum sensitivity because traditional activation layer materials such as Cs-O₂ and Cs-NF₃ form about a monolayer that is weakly bound to the surface and is chemically reactive.^{18,19} Enhancement of activation layer chemical stability has been shown by using two alkali species, Cs and Li, during activation.^{20–22} While the chemical reactivity is responsible for QE degradation when no photoemission is occurring (dark lifetime), the ion back-bombardment effect also limits the lifetime of the GaAs-based photocathodes during beam extraction. Deflecting the electron beam near the emission site was proposed to counteract this mechanism and showed an improvement in lifetime of both GaAs and alkali antimonide photocathodes.^{23–26}

Although *n*-type Cs₃Sb and CsI were demonstrated to be alternative activation materials at the time of the discovery of NEA activation,^{27–31} they have generally been avoided in the photocathode community because the semiconductor activation layer is thicker, and can potentially decrease spin polarization. Recent studies reported successful NEA activation on bulk GaAs using Cs₂Te,^{32–34} a semiconductor known for being a robust solar blind photocathode material itself.³⁵ It was demonstrated that Cs₂Te activation layer can improve the charge extraction lifetime by a factor of 5 without negatively affecting the spin polarization.³⁶ Yet, all experiments were done with bulk GaAs which only has up to 40% spin polarization at the room temperature, and semiconductor activation of high spin polarization photocathodes (like GaAs/GaAsP superlattice) and its effect on the degree of polarization have not been demonstrated.

Based on the heterojunction model, a semiconductor layer capable of NEA activation on *p*-type GaAs should satisfy two conditions (see Fig. 1): (i) the energy difference between the Fermi level and vacuum level should be smaller than the band gap of GaAs (1.42 eV) to achieve NEA, and (ii) the band gap of activation layer should be greater than that of GaAs to ensure transparency to photons with the GaAs band gap energy. Cs₃Sb has a band gap of 1.6 eV and small electron affinity of 0.45 eV. Such a small electron affinity hints at the possibility of NEA activation on GaAs using Cs₃Sb: as shown in Fig. 1, Cs₃Sb satisfies the two conditions mentioned above without any doping control.

Recently, Ref. 37 reported NEA activation on GaAs surfaces with Cs, Sb, and O₂ codeposited layer and changes in photocathode parameters as the thickness was varied. In this work, we demonstrate NEA conditions achieved on bulk *p*-type GaAs with Cs-Sb using various methods of oxygen exposure and its effect on photocathode parameters such as the lifetime, QE, and the degree of spin polarization. Then, a GaAs/GaAsP superlattice sample was activated with one of the methods (codeposition of Cs, Sb, and O₂) and compared with typical Cs-O₂ activation. We find a significant improvement in the lifetime at 780 nm while preserving 90% spin polarization.

II. GROWTH

$10 \times 10 \text{ mm}^2$ samples are prepared by cutting highly *p*-doped ($\text{Zn } 5 \times 10^{18} \text{ cm}^{-3}$) GaAs (100) wafers in air with a diamond scribe. Samples are then solvent cleaned with isopropanol and rinsed in de-ionized water. Wet-etching was later performed for each sample with 1% HF for 30 s to remove the native oxide layer with minimal surface damage.^{38,39} Samples were finally rinsed again in de-ionized water and then moved into vacuum. The growth chamber has Cs and Sb effusion cells installed under ultra-high vacuum (UHV) of $\sim 10^{-9}$ Torr. Shutters in front of each effusion cell control the flux on the sample surface. A leak valve connected to an oxygen bottle was used to leak oxygen into the chamber during

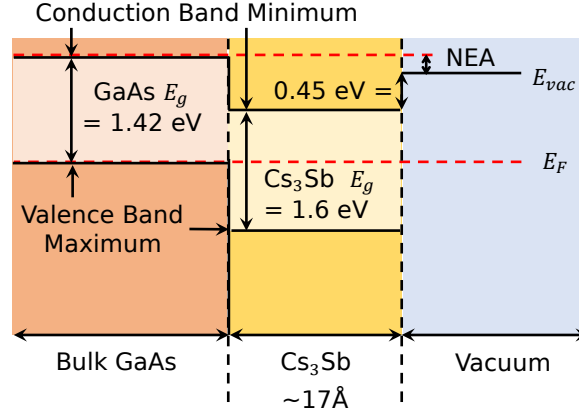


FIG. 1. Energy band diagram of GaAs activated with Cs_3Sb coating. An alternative activation layer needs to satisfy two conditions to achieve NEA. (i) The energy difference between the vacuum level E_{vac} and Fermi level E_F should be smaller than the GaAs band gap. (ii) The band gap of activation layer should be larger than the GaAs band gap so that the activation layer is transparent for photon energy near the GaAs band gap.

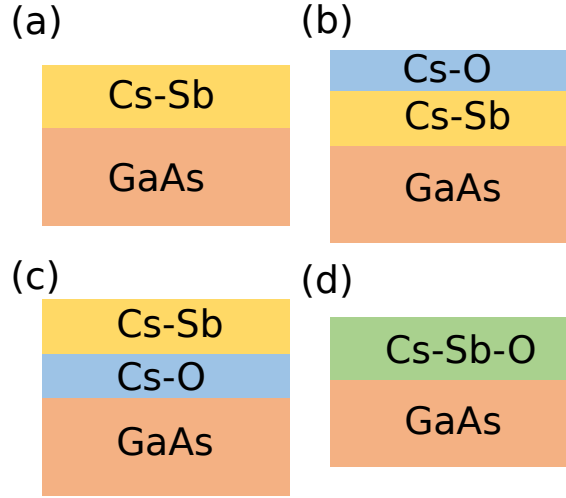


FIG. 2. Deposition order of different oxygen exposure methods used in Cs-Sb semiconductor activation. (a)-(d) represents methods (a)-(d) in the text.

the growths. Total pressure is monitored with a cold cathode gauge. GaAs samples were heat cleaned at $\sim 500^\circ\text{C}$ for about 12 hours. Then temperature was lowered to about 130°C for the growth. The same heat cleaning procedure was employed to prepare the reference sample which was later activated with Cs and O_2 at room temperature.

A 780 nm diode laser was used to excite the samples⁴⁰ that were biased at -18 V during the growth. This wavelength is at the NEA GaAs threshold. The drain current was measured via a lock-in amplifier locked to the frequency of an optical chopper used to modulate the laser light. Samples were grown with five different methods:

- (a) Cs and Sb are codeposited on GaAs without oxygen exposure.
- (b) Cs- O_2 codeposition was additionally performed after Cs-Sb codeposition to study the

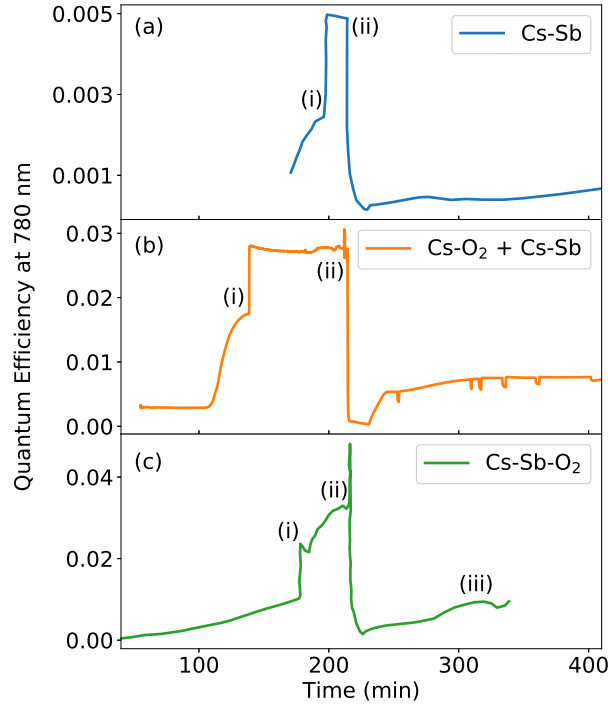


FIG. 3. Quantum Efficiency of GaAs photocathodes during the thin film growths. The initial QE at 780 nm is not zero due to residual cesium vapor in the growth chamber. The Cs shutter and Sb shutter are opened at (i) and (ii), respectively. (a) Oxygen was not used during the growth. (b) Oxygen was leaked before deposition of Sb. (c) Cs, Sb, and O_2 are codeposited during the growths. Oxygen leak valve was closed at (iii).

- effect of Cs- O_2 dipole layer on the surface.
- (c) Cs and O_2 are codeposited before the growth Cs-Sb to study the effect of Cs- O_2 dipole layer at the interface between GaAs and Cs-Sb layer.
- (d) Cs and Sb are codeposited under O_2 exposure throughout the growth procedure.
- (e) Conventional codeposition of Cs and O_2 was performed for a control sample.

Figure 2 illustrates the layer order for samples grown with Sb.

In Fig. 3, the QEs estimated during the different growth procedures of Cs-Sb on bulk GaAs with and without the oxygen exposure are plotted. At the beginning of the growth procedures, we found the samples already photoemitting at 780 nm. We attribute this to the Cs vapors already present in the UHV chamber from previous growth experiments. As the Cs furnace temperature is raised with the shutter closed, the QE increases further, likely because Cs vapors can make it through the gap between the shutter and furnace. In Fig. 3, (i) indicates the opening of the Cs shutter and (ii) is when the Sb shutter is opened. For all methods, the Sb shutter was left opened for 1000 seconds to deposit 2.5 \AA with a flux of $8.3 \times 10^{11} \text{ atoms/cm}^2/\text{s}$. Assuming Cs_3Sb single crystal structure, this amount of Sb corresponds to the total film thickness of 17 \AA .⁴¹ The Cs shutter was left open during the Sb layer deposition and the final cooling of the sample down to 50°C . The photocurrent showed a sudden increase as the Cs shutter is opened and rapid decrease when Sb shutter is opened. For the samples of Fig. 3 (a), no oxygen was leaked into the growth chamber (methods (a) and (b)). Oxygen was supplied with a partial pressure of $\sim 5 \times 10^{-9} \text{ Torr}$ in Fig. 3 (b) and (c); the leak valve was closed just before opening the Sb shutter in (b) (method (c)) and during cooling down (iii) in (c) (method (d)). The sample activated with method (b) was

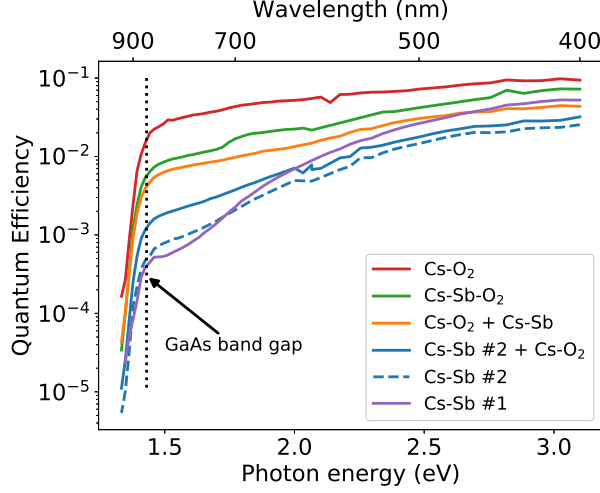


FIG. 4. Spectral response of GaAs samples activated by Cs, Sb, and O_2 using different methods. All samples indicate NEA activation on the surface by photoemission at GaAs band gap energy (1.42 eV).

moved under UHV into another chamber (with a base pressure of $\sim 5 \times 10^{-11}$ Torr) to be further activated by exposing simultaneously to Cs and O_2 at room temperature. For the superlattice sample, Cs, Sb, and O_2 are codeposited for activation as in Fig. 3 (c). Half the amount of Sb was deposited compared to the bulk samples (1.25 Å Sb and 8.5 Å total thickness) to maintain the spin polarization.³⁷

III. RESULTS

The spectral response of samples with different growth methods are reported in Fig. 4. Photoemission at the GaAs band gap photon energy (1.42 eV) confirms NEA achievement on the surface for all of the investigated activation methods. The reference sample, activated with Cs and O_2 , has the highest QE across the measured spectral range. The sample activated with only Cs-Sb has the lowest QE in the infrared region (about 2 orders of magnitude lower than the Cs- O_2 activated sample at 780 nm). Exposing to Cs- O_2 after or before the growth of the Cs-Sb layer (methods (b) and (c)) increases the QE near the GaAs bandgap energy: in particular for the sample prepared with method (c), we observed an increase of QE by about an order of magnitude with respect to the bare Cs-Sb activated sample. Finally, the Cs-Sb- O_2 codeposited sample (method (d)) showed the highest QE near the photoemission threshold among Sb-containing samples. These results illustrate the significance of the Cs- O_2 dipole layer in enhancing the NEA at the GaAs interface.

The robustness of the activating layers was compared by measuring the QE degradation over time. The lifetime of a photocathode is defined as the time QE takes to drop by a factor of e , the base of the natural logarithm.^{23,36} Photocurrent was measured continuously in the range of 1 - 100 nA with a 505 nm diode laser ($\sim 20 \mu W$) in Fig. 5. The Lifetime extracted from these measurements represent a convolution of the QE degradation from chemical poisoning (known as dark lifetime) and ion back-bombardment (known as charge lifetime). A detailed study of dark lifetime and charge extraction lifetime of codeposited samples is reported in Ref. 37.

From the data reported in Fig. 5, it can be seen that Sb deposited samples have at least a factor of 2.6 improvement in lifetime compared to the sample activated with Cs and O_2 . The longest lifetime (770 h) was observed when bare Cs-Sb is used for activation, but this method yielded the lowest efficiency near the threshold (Fig. 4). One order of magnitude increase

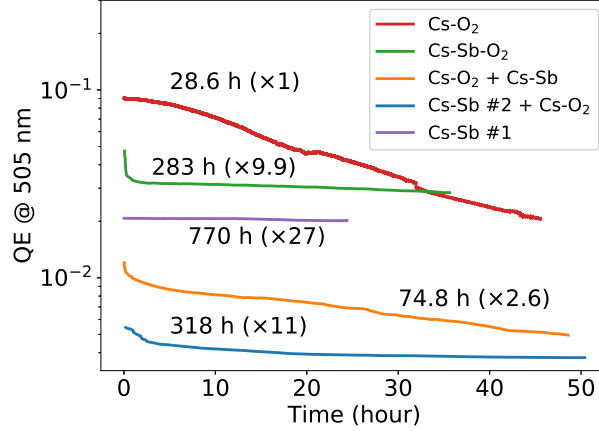


FIG. 5. Quantum Efficiency degradation as a function of time. 505 nm laser was used to illuminate the sample. The number next to each curve is the lifetime calculated by fitting each curve to an exponential function. Improvement factors from the standard Cs-O₂ activation are in the parentheses.

Activation method	Initial QE at 780 nm	Final QE at 780 nm	Lifetime estimate (hour)	Improvement factor
Cs-O ₂	3.3×10^{-2}	1.4×10^{-3}	15	$\times 1$
Cs-O ₂ + Cs-Sb	9.5×10^{-3}	2.9×10^{-3}	41	$\times 2.7$
Cs-Sb + Cs-O ₂	3.8×10^{-3}	1.1×10^{-3}	70	$\times 4.6$
Cs-Sb-O ₂	1.0×10^{-2}	7.0×10^{-3}	104	$\times 6.8$

TABLE I. Lifetimes at 780 nm estimated by comparing initial QE and final QE after the QE degradation measurement in Fig. 5.

in lifetime (~ 300 h) was observed when the samples are exposed to oxygen either after or during Cs-Sb growths. Table I reports estimated lifetimes at 780 nm. Spectral response at 780 nm was measured before and after the QE degradation measurement in Fig. 5, and the lifetime is calculated assuming an exponential decrease as a function of time between the two measured points. The Cs-Sb-O₂ activation showed the greatest improvement from Cs-O₂ activation by a factor of 6.8. As opposed to Cs₂Te activation, which showed a rapid increase of the work function as a function of time,³² the Cs-Sb-O₂ layer achieves significant enhancement in lifetime near the photoemission threshold.

Spin polarization of photoemitted electrons was measured by the Mott polarimeter described in Refs. 36 and 42. Monochromatic light was used to produce circularly polarized light directed at normal incidence to the sample surface. Longitudinally spin polarized electrons were bent 90° by electrostatic lenses and Mott scattered with 20 keV at a tungsten target which was calibrated to have 0.18 Sherman function.^{36,42} Photoelectron spin polarization was measured as a function of wavelength for each sample in Fig. 6. The maximum spin polarization varied up to 5% which corresponds to about 3 standard deviations. The detailed study³⁷ on the samples activated with the Cs-Sb-O₂ method reveals a significant spin depolarization as thickness of the Sb layer grows.

Since the Cs-Sb-O₂ codeposited sample showed both the highest QE at the photoemission threshold among Sb deposited samples and a significantly improved lifetime, we chose the codeposition method to activate a GaAs/GaAsP superlattice sample⁴³ (Fig. 7). Compared to the bulk samples, a half the amount of Sb is deposited (1.25 Å) to minimize depolarization at the activation layer.³⁷ Both samples showed ~ 90 % maximum spin polarization with agreement within one standard deviation. The QE at 780 nm was a factor of 3 smaller

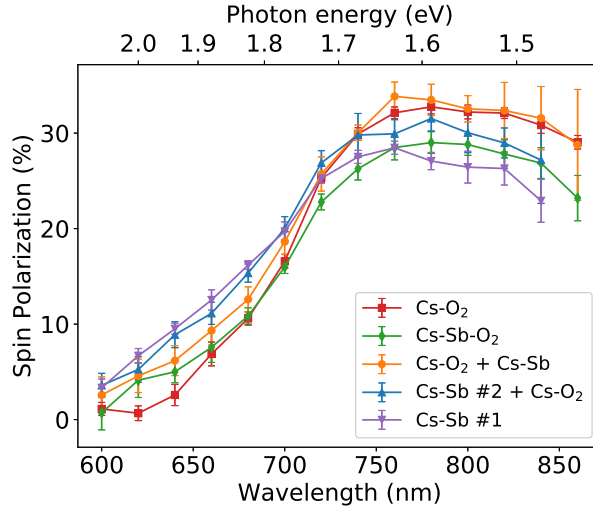


FIG. 6. Spin polarization of photoemitted electron from GaAs activated by Cs, Sb, and O₂.

for the semiconductor activated sample. QE was continuously measured in Fig. 7 (b) for lifetime estimation at 780 nm, the wavelength commonly used for a highly spin polarized photoemission. The lifetime showed a factor of 7 improvement, which is similar to the bulk results in Table. I that were activated with twice the amount of Sb.

IV. DISCUSSION

The sample prepared with method (c) (where the Cs-O₂ is deposited on the surface of GaAs under the Cs-Sb layer) has a higher QE than the sample prepared with method (b), where the Cs-O₂ is deposited above the Cs-Sb layer. This suggests that despite the small thickness of the activating layers, segregation can take place such that the intermediate Cs-O₂ layer retains the strong electric dipole enhancing the transmission from GaAs into the Cs-Sb layer. Additionally, the QE near threshold of the sample exposed to Cs-O₂ after depositing Cs-Sb is larger than the one activated only with Cs-Sb. Studies on the nature of the GaAs/Cs-O activation layer indicate that the dipole layer consists of a Cs⁺-O²⁻-Cs⁺ sandwich on a O-GaAs layer, and the strong double dipole layer results in a higher QE compared to Cs only activation.¹³ On the other hand, studies on the oxidation of alkali antimonide photocathodes show that, during oxidation, the films segregate in a alkali-oxide rich surface layer on top of the alkali antimonide layer.⁴⁴ In particular, at low oxygen exposures (less than 10 L for Cs_{2.5}K_{0.5}Sb),⁴⁴ the top surface is mainly composed of a Cs suboxide (Cs₁₁O₃)⁴⁵ that is known to promote photoemission, in particular at long wavelengths.⁴⁶

The above discussion suggests that the sample activated with Cs-Sb-O₂ should indeed have the the largest QE among the alternative methods. In this case, the continuous oxygen exposure can result in the formation of strong electric dipole at both the interface with GaAs and at the surface of Cs-Sb that can favor both electron tunneling from GaAs to Cs-Sb and electron emission from Cs-Sb to vacuum. The oxygen dosed on the samples during codeposition can be estimated to be of the order of 50 L - 75 L; since Cs is provided during the oxygen exposure and after the closure of the oxygen leak valve, it is reasonable to expect the formation of Cs-rich suboxides on the sample surface.

Photoexcited electrons experience a potential barrier at the GaAs surface in the process of emission into the vacuum. Although various models of the potential barrier were proposed, fundamental understanding of the nature of the barrier is lacking.^{48,49} Rectangular,⁵⁰ triangular,⁴⁷ quadratic,⁵¹ and double triangular⁴⁹ shapes have been proposed in previous

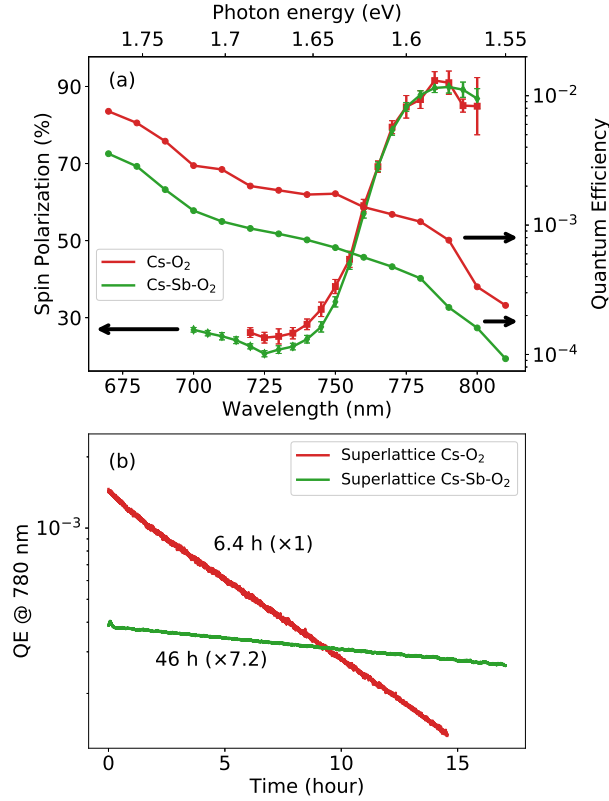


FIG. 7. Spin polarization, quantum efficiency, and lifetime measurement of GaAs/GaAsP superlattice sample activated by codeposition of Cs-Sb-O₂ and standard Cs-O₂.

studies to reproduce various experimental observations. In Fig. 8, a simple potential barrier was constructed to numerically investigate how different methods of oxygen exposure during Cs-Sb growths can affect the shape of the potential barrier and QE as a result.

In the bulk of GaAs, we implement quadratic band-bending near the surface with a 100 Å band bending region and 0.4 eV band bending magnitude.⁴⁸ A simple triangular potential barrier was placed at the interface between GaAs and the activation layer. The height of the triangle was fixed at 4 eV above the conduction band minimum (CBM) of GaAs⁴⁷ while the width was varied throughout the simulations. The variation of the width can be interpreted as a change in dipole moment strength at the interface. The bottom of the potential well between the triangular barrier and the vacuum interface was fixed at 0.35 eV below the conduction band minimum.^{49,52,53} The vacuum interface is positioned at 17 Å from the GaAs surface which is the estimated thickness of the activation layer.

The transmission probabilities (P) of constructed potential barriers are calculated by the propagation matrix approach^{48,54,55} and used to compute QE numerically with the following equation:⁵⁶

$$QE = (1 - R)F \frac{\int_0^\infty dE f(E) \int_0^1 d(\cos \theta) P(E \cos^2 \theta)}{\int_0^\infty dE f(E) \int_{-1}^1 d(\cos \theta)}. \quad (1)$$

Here, R is the optical reflectance of GaAs, F is a scattering contribution (from holes, impurities, and phonons)⁴⁸ which can be approximated to be independent of energy near the photoemission threshold,⁵⁶ θ is the angle between the electron velocity and the surface

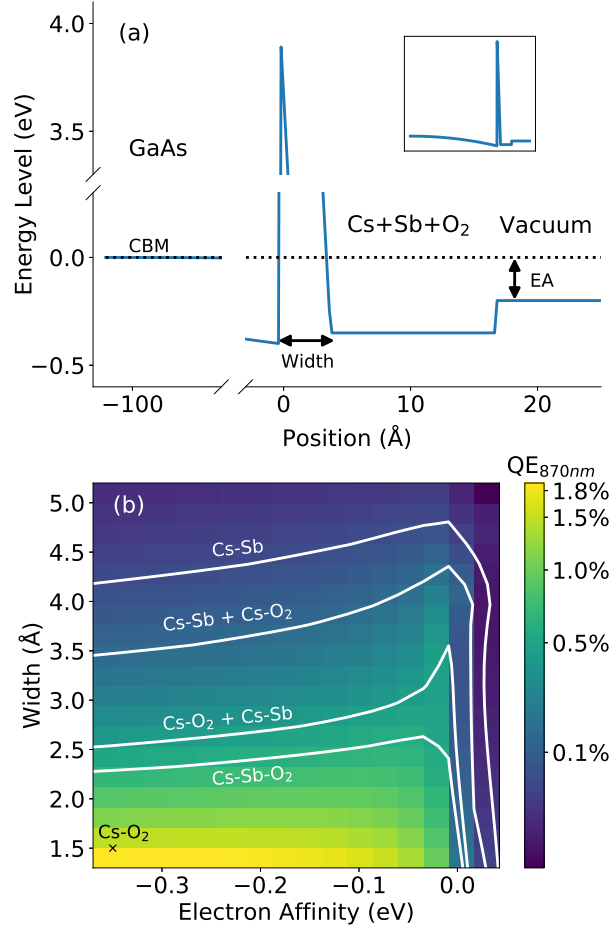


FIG. 8. Numerical simulation of quantum efficiency under various potential barrier shapes. (a) Potential barriers were constructed for 17 Å thick semiconductor activation layer to calculate transmission probabilities. (b) Width and EA are varied to compute threshold QE. The black mark corresponds to the standard Cs-O₂ activation sample. Potential barrier parameters in Ref. 47 were used. White contour lines are sets of parameters that reproduce experimentally measured QEs.

normal, and $f(E)$ is a Fermi-Dirac distribution of photoexcited electrons:

$$f(E) = \frac{1}{1 + e^{[E - (h\nu - E_g)]/kT}} \quad (2)$$

where $h\nu$ is the photon energy, E_g is the GaAs band gap, k is the Boltzmann constant, and T is the room temperature. Additional scatterings at the semiconductor activation layer can be considered mostly elastic electron-electron collisions, therefore it is ignored.³⁷

In Fig. 8 (b), QEs are calculated for various sets of the triangle width and electron affinity. The photoemission threshold wavelength 870 nm was used, and the scattering term F was set to be 0.21 to match the experimentally measured value of Cs-O₂ activated sample to the calculated one. The width of triangular potential barrier of Cs-O₂ activation layer is reported to be 1.5 Å⁴⁷ with 0.35 eV NEA.^{49,52,53} The white contour line for each growth method represent the set of parameters that reproduce the experimentally measured QE at 870 nm. The contour lines suggest when NEA is greater than 0.1 eV, the efficiency is roughly independent of NEA while the barrier width plays critical role on QE. Considering that a small width represents strong dipole moment on the surface, activation with oxygen at the interface between bulk GaAs and activation layer is essential to achieve a high QE.

Thus, this simple model can explain why samples activated with oxygen before and during the Cs-Sb growth showed greater improvement in QE compared to the sample exposed to oxygen after Sb deposition which is related to greater NEA at the vacuum interface.

V. CONCLUSION

We have investigated the NEA activation of GaAs samples with Cs, Sb and O₂ in various recipes. Of the recipes attempted, we found that the codeposition method can achieve the highest QE ($\sim 1\%$ at 780 nm) with a factor of 10 and 7 improvement in lifetime at 505 nm and 780 nm, respectively, compared to the conventional Cs-O₂ activation. Similar results were obtained for the high polarization GaAs/GaAsP superlattice sample. This sample showed a factor of 7 improvement in lifetime at 780 nm without any depolarization at a cost of a factor of 3 smaller QE. A simple numerical model was proposed to estimate QE for various shapes of the potential barrier at the relatively thick semiconductor activation layer. According to the model, the dipole moment strength at the GaAs interface with the activation layer is critical to achieve a high QE at the photoemission threshold. This explains the significant improvement in QE we observed when the samples were exposed to oxygen before activation layer growths.

Future work will involve surface characterization of the activation layer to understand the chemical and structural composition. This information can be used to properly model the heterojunction band structures with density functional theory. Monte Carlo techniques can be considered to model the electron spin transport and to study the depolarization mechanisms. Furthermore (and perhaps most critically), we plan to test the performance of these unconventional activation layers in a real high voltage, high current DC gun environment in the future.

VI. ACKNOWLEDGMENTS

This work was supported by the Department of Energy under Grant No. de-sc0019122 and National Science Foundation under Grant No. PHY-1549132. Authors would like to acknowledge Marcy Stutzman, Matt Poelker, Joe Grames, and William DeBenedetti for valuable discussions, help in preparing GaAs samples, and providing GaAs/GaAsP superlattice samples.

¹Report of the Community Review of EIC Accelerator R&D for the Office of Nuclear Physics, 2017.

²Reaching for the Horizon: The 2015 Long Range Plan for Nuclear Science, 2015.

³Major Nuclear Physics Facilities for the Next Decade: Report of the NSAC Subcommittee on Scientific Facilities, 2013.

⁴*An Assessment of U.S.-Based Electron-Ion Collider Science*. 2018.

⁵Masahiko Suzuki, Michihiro Hashimoto, Tsuneo Yasue, Takanori Koshikawa, Yasuhide Nakagawa, Taro Konomi, Atsushi Mano, Naoto Yamamoto, Makoto Kuwahara, Masahiro Yamamoto, Shoji Okumi, Tsutomu Nakanishi, Xiuguang Jin, Toru Ujihara, Yoshikazu Takeda, Teruo Kohashi, Takashi Ohshima, Takashi Saka, Toshihiro Kato, and Hiromichi Horinaka. Real time magnetic imaging by spin-polarized low energy electron microscopy with highly spin-polarized and high brightness electron gun. *Applied Physics Express*, 3(2):6–9, 2010.

⁶M. Kuwahara, S. Kusunoki, X. G. Jin, T. Nakanishi, Y. Takeda, K. Saitoh, T. Ujihara, H. Asano, and N. Tanaka. 30-kV spin-polarized transmission electron microscope with GaAs-GaAsP strained superlattice photocathode. *Applied Physics Letters*, 101(3), 2012.

⁷R. Vollmer, M. Etzkorn, P. S. Anil Kumar, H. Ibach, and J. Kirschner. Spin-polarized electron energy loss spectroscopy of high energy, large wave vector spin waves in ultrathin fcc co films on cu(001). *Physical Review Letters*, 91(14):1–4, 2003.

⁸Wei Liu, Yiqiao Chen, Wentao Lu, Aaron Moy, Matthew Poelker, Marcy Stutzman, and Shukui Zhang. Record-level quantum efficiency from a high polarization strained GaAs/GaAsP superlattice photocathode with distributed Bragg reflector. *Applied Physics Letters*, 109(25), 2016.

⁹Lawrence S. Cardman. The PEPPo method for polarized positrons and PEPPo II. *AIP Conference Proceedings*, 1970(May), 2018.

¹⁰J. J. Scheer and J. van Laar. GaAs-Cs: A new type of photoemitter. *Solid State Communications*, 3(8):189–193, 1965.

- ¹¹Wei Liu, Matt Poelker, Xincun Peng, Shukui Zhang, and Marcy Stutzman. A comprehensive evaluation of factors that influence the spin polarization of electrons emitted from bulk GaAs photocathodes. *Journal of Applied Physics*, 122(3):0–9, 2017.
- ¹²Daniel Pierce and Felix Meier. Photoemission of spin-polarized electrons from GaAs. *Physical Review B*, 13(12), 1976.
- ¹³C. Y. Su, W. E. Spicer, and I. Lindau. Photoelectron spectroscopic determination of the structure of (Cs,O) activated GaAs (110) surfaces. *Journal of Applied Physics*, 54(3):1413–1422, 1983.
- ¹⁴Franco Ciccacci and Gualtiero Chiaia. Comparative study of the preparation of negative electron affinity GaAs photocathodes with O₂ and with NF₃. *Journal of Vacuum Science & Technology A: Vacuum, Surfaces, and Films*, 9(6):2991, 1991.
- ¹⁵N. B. Clayburn, J. L. McCarter, J. M. Dreiling, M. Poelker, D. M. Ryan, and T. J. Gay. Search for spin-polarized photoemission from GaAs using light with orbital angular momentum. *Physical Review B - Condensed Matter and Materials Physics*, 87(3):1–8, 2013.
- ¹⁶J. L. McCarter, A. Afanasev, T. J. Gay, J. Hansknecht, A. Kechiantz, and M. Poelker. Measurement of electron beam polarization from unstrained GaAs via two-photon photoemission. *Nuclear Instruments and Methods in Physics Research, Section A: Accelerators, Spectrometers, Detectors and Associated Equipment*, 738:149–153, 2014.
- ¹⁷T Maruyama, E L Garwin, R Prepost, and G H Zapalac. Electron-spin polarization in photoemission from strained GaAs grown on GaAs 1-x P x. *Physical Review B*, 46(7):4261–4264, 1992.
- ¹⁸M. Kuriki, C. Shonaka, H. Iijima, D. Kubo, H. Okamoto, H. Higaki, K. Ito, M. Yamamoto, T. Konomi, S. Okumi, M. Kuwahara, and T. Nakanishi. Dark-lifetime degradation of GaAs photo-cathode at higher temperature. *Nuclear Instruments and Methods in Physics Research, Section A: Accelerators, Spectrometers, Detectors and Associated Equipment*, 637(1 SUPPL.):S87–S90, 2011.
- ¹⁹N. Chanlek, J. D. Herbert, R. M. Jones, L. B. Jones, K. J. Middleman, and B. L. Militsyn. The degradation of quantum efficiency in negative electron affinity GaAs photocathodes under gas exposure. *Journal of Physics D: Applied Physics*, 47(5), 2014.
- ²⁰G. A. Mulhollan and J. C. Bierman. Enhanced chemical immunity for negative electron affinity GaAs photoemitters. *Journal of Vacuum Science & Technology A: Vacuum, Surfaces, and Films*, 26(5):1195–1197, 2008.
- ²¹Y. Sun, R. E. Kirby, T. Maruyama, G. A. Mulhollan, J. C. Bierman, and P. Pianetta. The surface activation layer of GaAs negative electron affinity photocathode activated by Cs, Li, and NF₃. *Applied Physics Letters*, 95(17), 2009.
- ²²N Kurichyanil, J Enders, Y Fritzsche, and M Wagner. A test system for optimizing quantum efficiency and dark lifetime of gaas photocathodes. *Journal of Instrumentation*, 14(08):P08025, 2019.
- ²³J. Grames, R. Suleiman, P. A. Adderley, J. Clark, J. Hansknecht, D. MacHie, M. Poelker, and M. L. Stutzman. Charge and fluence lifetime measurements of a dc high voltage GaAs photogun at high average current. *Physical Review Special Topics - Accelerators and Beams*, 14(4):1–12, 2011.
- ²⁴R. R. Mammei, R. Suleiman, J. Feingold, P. A. Adderley, J. Clark, S. Covert, J. Grames, J. Hansknecht, D. Machie, M. Poelker, T. Rao, J. Smedley, J. Walsh, J. L. McCarter, and M. Ruiz-Osés. Charge lifetime measurements at high average current using a K₂CsSb photocathode inside a dc high voltage photogun. *Physical Review Special Topics - Accelerators and Beams*, 16(3):1–16, 2013.
- ²⁵Omer Rahman, Erdong Wang, Ilan Ben-Zvi, Jyoti Biswas, and John Skaritka. Increasing charge lifetime in DC polarized electron guns by offsetting the anode. 2019.
- ²⁶Luca Cultrera, Jared Maxson, Ivan Bazarov, Sergey Belomestnykh, John Dobbins, Bruce Dunham, Sidharth Karkare, Roger Kaplan, Vaclav Kostroun, Yulin Li, Xianghong Liu, Florian Löhl, Karl Smolenski, Zhi Zhao, David Rice, Peter Quigley, Maury Tigner, Vadim Veshcherevich, Kenneth Finkelstein, Darren Dale, and Benjamin Pichler. Photocathode behavior during high current running in the Cornell energy recovery linac photoinjector. *Physical Review Special Topics - Accelerators and Beams*, 14(12):1–9, 2011.
- ²⁷H. Sonnenberg. Low-work-function surfaces for negative-electron-affinity photoemitters. *Applied Physics Letters*, 14(9):289–291, 1969.
- ²⁸H. Sonnenberg. Related content On Photoemission from GaAs Cs Sb. *Japan. J. Appl. Phys.*, 8:806, 1969.
- ²⁹Minoru Hagino and Ryoza Nishida. Related content Photoemission from GaAs-Cs-Sb (Te). *Jpn. J. Appl. Phys.*, 8:123, 1969.
- ³⁰Libin Zhao, Qing Zhou, Shouzhen Zhao, and Baoseng Xie. Study of GaAs-Cs-Sb photoemitter. (April 1993):140–144, 1993.
- ³¹Tailiang Guo. Novel GaAs photocathodes with alkali antimonide intermediate layers and caesium-oxygen adlayers. *Thin Solid Films*, 281-282(1-2):379–382, 1996.
- ³²H. Sugiyama, K. Ogawa, J. Azuma, K. Takahashi, M. Kamada, T. Nishitani, M. Tabuchi, T. Motoki, K. Takashima, A. Era, and Y. Takeda. A study of an electron affinity of cesium telluride thin film. *Journal of Physics: Conference Series*, 298(1), 2011.
- ³³K Uchida, M Kuriki, Y Seimiya, R Kaku, K Miyoshi, and N Yamamoto. A Study on Robustness of NEA-GaAs Photocathode. *Proceedings of IPAC2014*, pages 664–666, 2014.
- ³⁴M. Kuriki, Y. Seimiya, K. Uchida, and S. Kashiwagi. GaAs photocathode activation with CsTe thin film. *6th International Particle Accelerator Conference, IPAC 2015*, pages 2–4, 2015.
- ³⁵P Michelato, C Pagani, D Sertore, Infm Milano Lasa, I-Segrata Mi, F Stephan, Desy Zeuthen, S Lederer, S Schreiber, and Desy Hamburg. Cs 2 Te PHOTOCATHODES ROBUSTNESS STUDIES *. *Proceedings*

- of EPAC08, (Mi):241–243, 2008.
- ³⁶Jai Kwan Bae, Luca Cultrera, Philip Digiaco, and Ivan Bazarov. Rugged spin-polarized electron sources based on negative electron affinity GaAs photocathode with robust Cs₂Te coating. *Applied Physics Letters*, 112(15):1–6, 2018.
- ³⁷L. Cultrera. 2019. Submitted.
- ³⁸M. Rei Vilar, J. El Beghdadi, F. Debontridder, R. Artzi, R. Naaman, A. M. Ferraria, and A. M Botelho Do Rego. Characterization of wet-etched GaAs (100) surfaces. *Surface and Interface Analysis*, 37(8):673–682, 2005.
- ³⁹Cheng Feng, Yijun Zhang, Jian Liu, Yunsheng Qian, Jingzhi Zhang, Jing Zhao, Feng Shi, and Xiaofeng Bai. Optimized chemical cleaning procedure for enhancing photoemission from GaAs photocathode. *Materials Science in Semiconductor Processing*, 91(June 2018):41–46, 2019.
- ⁴⁰Cheng Feng, Yijun Zhang, Yunsheng Qian, Jian Liu, Jingzhi Zhang, Feng Shi, Xiaofeng Bai, and Jijun Zou. Improved quantum efficiency and stability of GaAs photocathode using favorable illumination during activation. *Ultramicroscopy*, 202(April):128–132, 2019.
- ⁴¹Minoru Hagino and Tadashi Takahashi. Thickness of Cs-Sb films relative to the original Sb films. *Journal of Applied Physics*, 37(10):3741–3743, 1966.
- ⁴²G. A. Mulhollan. Low-energy polarized electron source test facilities. Technical report, 1994.
- ⁴³T. Maruyama, D. A. Luh, A. Brachmann, J. E. Clendenin, E. L. Garwin, S. Harvey, J. Jiang, R. E. Kirby, C. Y. Prescott, R. Prepost, and A. M. Moy. Systematic study of polarized electron emission from strained GaAs/GaAsP superlattice photocathodes. *Applied Physics Letters*, 85(13):2640–2642, 2004.
- ⁴⁴Leonardo Soriano and Luis Galán. Interaction of Cesium-Potassium Antimonide Photocathode Materials with Oxygen: an X-Ray Photoelectron Spectroscopy Study. *Japanese Journal of Applied Physics*, 32(Part 1, No. 10):4737–4744, oct 1993.
- ⁴⁵A. Galdi, W.J.I. DeBenedetti, J. Balajka, L. Cultrera, M. A. Hines, S. A. McBride, J. B. Baretz, F. Ikponwmen, I. V. Bazarov, and J. M. Maxson. Towards the optimization of photocathode properties via surface science techniques: A study on cs₃sb thin film growth. *Proceedings of NAPAC'19*, page MOPLH24, 2019.
- ⁴⁶C. W. Bates, Th. M. van Atekum, G. K. Wertheim, D. N. E. Buchanan, and K. E. Clements. X-ray photoemission studies of superficially oxidized cesium antimonide photoemitters. *Applied Physics Letters*, 38(5):387–389, 1981.
- ⁴⁷G. Vergara, A. Herrera-Gómez, and W. E. Spicer. Calculated electron energy distribution of negative electron affinity cathodes. *Surface Science*, 436(1):83–90, 1999.
- ⁴⁸Siddharth Karkare, Dimitre Dimitrov, William Schaff, Luca Cultrera, Adam Bartnik, Xianghong Liu, Eric Sawyer, Teresa Esposito, Ivan Bazarov, Siddharth Karkare, Dimitre Dimitrov, William Schaff, Luca Cultrera, and Adam Bartnik. Monte Carlo charge transport and photoemission from negative electron affinity GaAs photocathodes. *Journal of Applied Physics*, 113(104904):2015–2017, 2013.
- ⁴⁹Xiuguang Jin, Alexandre A.C. Cotta, Gong Chen, Alpha T. N'Diaye, Andreas K. Schmid, and Naoto Yamamoto. Low energy electron microscopy and Auger electron spectroscopy studies of Cs-O activation layer on p-type GaAs photocathode. *Journal of Applied Physics*, 116(17), 2014.
- ⁵⁰D. G. Fisher, R. E. Enstrom, J. S. Escher, and B. F. Williams. Photoelectron surface escape probability of (Ga,In)As: CsSingle Bond signO in the 0.9 to [inverted lazy s] 1.6 μ m range. *Journal of Applied Physics*, 43(9):3815–3823, 1972.
- ⁵¹A.V. Subashiev and J.E. Clendenin. No Title. *Int. J. Mod. Phys. A*, 15(25), 2000.
- ⁵²J. J. Uebbing and L. W. James. Behavior of cesium oxide as a low work-function coating. *Journal of Applied Physics*, 41(11):4505–4516, 1970.
- ⁵³V. V. Bakin, K. V. Toropetsky, H. E. Scheibler, A. S. Terekhov, L. B. Jones, B. L. Militsyn, and T. C.Q. Noakes. P-GaAs(Cs,O)-photocathodes: Demarcation of domains of validity for practical models of the activation layer. *Applied Physics Letters*, 106(18):1–5, 2015.
- ⁵⁴Anthony Frederic John Levi. *Applied quantum mechanics*. Cambridge University Press, 2006.
- ⁵⁵Robert Gilmore. *Elementary quantum mechanics in one dimension*. JHU Press, 2004.
- ⁵⁶David H. Dowell and John F. Schmerge. Quantum efficiency and thermal emittance of metal photocathodes. *Physical Review Special Topics - Accelerators and Beams*, 12(7):1–10, 2009.